Danner and de Meer *Energy Informatics* 2022, **5**(Suppl 1):15
https://doi.org/10.1186/s42162-022-00211-w

Energy Informatics

RESEARCH Open Access

Max-consensus protocol to determine the regulated node in distributed voltage regulation

Dominik Danner* and Hermann de Meer

From The 11th DACH+ Conference on Energy Informatics 2022 Freiburg, Germany. 15-16 September 2022

*Correspondence:
dominik.danner@uni-passau.de

University of Passau, Innstraße 41, 94032 Passau, Germany

Abstract

Literature that deals with optimal voltage regulation in the power distribution grid often neglects the impact of communication on their control strategies or makes hard assumptions about the communication network. This paper extends a nearly optimal reactive power allocation mechanisms for distributed renewable energy sources with communication considerations and proposes a max-consensus-based communication schema to determine the regulated node in a distributed manner. The proposed consensus mechanisms is validated by co-simulation of a multi-agent system, the IEEE 906 low voltage test feeder and a simple communication simulator to evaluate the impact of message delay and communication network topology.

Keywords: Max-consensus problem, Voltage regulation, Smart grid, Co-simulation

Introduction

To achieve a carbon-neutral electricity system, Distributed Renewable Energy Sources (DRESs), such as Photovoltaics (PVs), are installed in the distribution grid. Especially in rural areas, additional PV generation can cause reverse power flow, which result in overvoltage situations. To avoid generation curtailment, DRESs can offer voltage regulation as Ancillary Service (AS) to the grid operator (Kryonidis et al. 2021; Rousis et al. 2021).

In literature, several papers propose centralized and decentralized solutions for optimal voltage regulation to achieve different goals such as fairness (Hu et al. 2021; Kryonidis et al. 2018) or loss minimization (Kryonidis et al. 2019, 2020, 2021; Faiya et al. 2021; Kontis et al. 2019; Millar and Jiang 2018). In Hu et al. (2021), the optimal active and reactive power allocation of electric vehicle charging is determined using a parallel consensus mechanisms to establish a local power dispatch. Their solution implements fair pricing schemes that use the involvement level of the individual vehicles. Authors of (Faiya et al. 2021) propose a self-organized Multi-Agent System (MAS) that clusters the distribution grid based on its sensitivity matrix and solves smaller optimization

problems centrally at *linear programming solver* agents. In Kryonidis et al. (2021), DRESs contribute reactive power in a coordinated, nearly-optimal manner by delaying their reactive power reaction according to the sensitivity matrix of the distribution system (Kryonidis et al. 2016), which minimizes grid losses. Consensus protocols are used for optimal power flow (Millar and Jiang 2018), management of virtual power plants (Wang et al. 2018), or more generally for various purposes in wireless sensor networks (Iutzeler et al. 2012). The impact of the communication topology and network delay on distributed voltage regulation is rarely addressed or are subject to hard assumptions.

This paper contributes with the following points:

- A new max-consensus protocol that determines the maximum voltage node (regulated node) of the power distribution grid in a fully decentralized manner, independent of the underlying communication network topology.
- Cross-disciplinary dynamic sensitivity ring overlay network design using the sensitivity matrix of the voltage controller.
- Comparison of different overlay networks in co-simulation on the IEEE 906 low voltage test feeder and a simple queuing-based communication simulator to validate the impact of message delay and communication topology.

Methodology

In general, there are *synchronous* and *asynchronous* max-consensus protocols, of which different aspects are discussed in literature, e.g., convergence (Giannini et al. 2013a, b, 2016; Lin et al. 2007; Shi et al. 2015), max-plus algebra (Nejad et al. 2009), or signal noise (Zhang et al. 2016). Additionally, they can be classified as *static* (constant signal) or *dynamic* (varying signal and/or number of agents). Although there exist methods to approximate the maximum of dynamic signals (Deplano et al. 2020; Monteiro and Peixoto 2020), this paper models varying input signals as a sequence of static max-consensus problems.

The voltage regulation algorithm is equal to the work by Kryonidis et al. (2021). They iteratively require a consensus on the maximum voltage in the grid, but do not analyze the effect of communication on their algorithm. This work extends the voltage regulation with communication aspects and the fully decentralized detection of the maximum voltage node. To clearly distinguish the systems, we use the terms *node* and *line* for the power system, *vertex* and *edge* for the communication system, and *agent* and *neighbor* for the MAS. All variables are summarized in Table 1.

Power system nodes (e.g., bus bars) are connected by lines (e.g., overhead cables) to form the power grid. The distributed algorithm (Kryonidis et al. 2021) solves overvoltage events with nearly minimum grid losses by utilizing reactive power capabilities of the DRES that is located nearest to the node with the highest measured voltage value, also called the *regulated node* (Kryonidis et al. 2019). Because low voltage grids have a high R/X ratio, the reaction of the local DRES might not be sufficient to fully mitigate the voltage violation, but other nearby DRESs can support. In order to minimize the grid losses, the approach of Kryonidis et al. (2021) selects the next best DRES according to the sensitivity matrix, which measures the impact of reactive

Table 1 Overview of voltage regulation, max-consensus and communication network variables

Variable	Description
$n \in \mathbb{N}$	Number of voltage measurement nodes
$d \leq n$	Number of DRES nodes
$\overline{Q}_i \in \mathbb{R}$	Reactive power limit of DRES i [VAr]
$Q_i < \overline{Q}_i$	Reactive power values of DRES i [VAr]
$\overline{U} \in \mathbb{R}$	Maximum allowed voltage value [V]
$db \in \mathbb{R}$	Dead-band below $\overline{U}$ [V]
$S \in \mathbb{R}^{n \times d}$	Sensitivity matrix
$d^{up} \in \mathbb{N}^{n \times d}$	Delay time up ($d^{up}_{j,i}$: DRES i and regulated node j)
$d^{down} \in \mathbb{N}^{n \times d}$	Delay time down
$\Delta^{delay} \in \mathbb{N}$	Delay time constant
$U^{loc} \in \mathbb{R}^n$	Local voltage values [V]
$U \in \mathbb{R}^n$	Known maximum voltage values [V]
$r \in \{1, \ldots, n\}^n$	Known regulated node at each agent
$t \in \mathbb{N}^n$	Node sequence numbers
$m_i = (U_i, r_i, t_{r_i})$	Information state at agent i, initially (U^{loc}_i, i, t_i)
$\Delta^{volt} \in \mathbb{N}$	Voltage measurement interval
$m \geq n$	Number of communication vertices
$\mathcal{V} = \{v_1, \ldots, v_m\}$	Communication vertex set
$\mathcal{E} \subseteq \mathcal{V} \times \mathcal{V}$	Edges connecting communication vertices
$\mathcal{G} = (\mathcal{V}, \mathcal{E})$	Communication network graph
$\mathcal{V}' \subseteq \mathcal{V}$	Consensus vertex set
$\mathcal{E}' \subseteq \mathcal{V}' \times \mathcal{V}'$	Edges connecting consensus vertices
$\mathcal{G}' = (\mathcal{V}', \mathcal{E}')$	Consensus overlay network graph
$\Delta^{com} \in \mathbb{N}$	Communication interval

power variations on the voltage at the regulated node. For a given voltage variation at a certain node, a DRES with higher sensitivity will need to absorb less reactive power than a DRES with lower sensitivity. Reactive power absorption in low voltage grids correlates with active power losses due to higher current flows. Consequently, selecting a DRES with high sensitivity and therefore low reactive power contribution will result in near-minimum power losses (Kryonidis et al. 2021).

It is assumed that all relevant nodes $k \in \{1, \ldots, n\}$ can measure local voltage values U^{loc}_k. Furthermore, DRESs exist at a subset of those nodes d, $1 \leq d \leq n$, which can control their reactive power with an upper limit of $\overline{Q}_k$. The flow chart in Fig. 1 shows a practical implementation of the distributed control scheme that is applied at each DRES node i.

First, the regulated node j with the maximum voltage is determined. Therefore, every node needs to measure its local voltage value and share this value with all other nodes such that every DRES can obtain $\max_{k=1,\ldots,n}(U^{loc}_k)$. More details on communication and distributed maximum value calculation are given in the following sections. If the maximum measured voltage $\max U^{loc}$ is greater than the maximum allowed voltage $\overline{U}$ (right branch of the flow chart), after a certain time delay reactive power is absorbed using a PI controller until one of the following conditions is met.

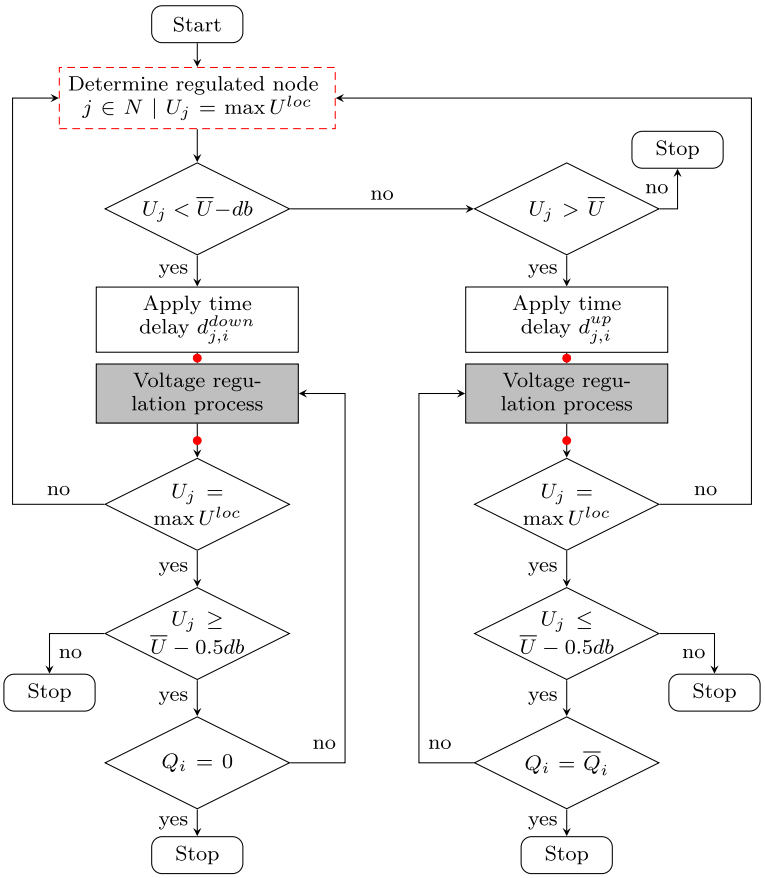

Fig. 1 Reactive power control scheme at DRES *i* according to Kryonidis et al. (2021). The Proportional Integral (PI) controller is part of the gray shaded voltage regulation process box. Note, that determination of the maximum voltage node (red dashed box) is also required after the delay time has elapsed and after the voltage regulation process (red dots on the arrows)

i. The regulated node changes from j to j'. In this case, the impact of DRES i on the voltage might differ and, therefore, a different time delay is applied. The process restarts with a new maximum voltage value at regulated node j'.
ii. The maximum reactive power at DRES i is reached. In this case, other DRESs will start absorbing reactive power after their delay time.
iii. The overvoltage is finally cleared and the voltage value at the regulated node resides below the maximum limit $\overline{U}$ minus half of the dead-band db to avoid oscillation caused by varying voltage profiles.

Similarly, in case the maximum voltage value is below the permissible limit (considering db), the regulation process reverses to release unnecessary reactive power from the grid. Before the PI controller starts absorbing reactive power, each DRES needs to wait a certain delay time ($d^{up}_{j,i}$ or $d^{down}_{j,i}$). This ensures that the DRESs start contributing in the optimal order to minimize power losses. The respective delay times are extracted from the sensitivity matrix of the power grid, which is calculated using the time-invariant line impedance (following the approach in Brenna et al. (2013)) instead of the inverse Jacobian matrix. In this way, the sensitivity matrix and thus

the corresponding delay times can be precomputed based on the power grid topology only. Both, the sensitivity matrix and the delay matrices contain row entries for each potential regulated node, but only sensitivity/delay values for all DRES nodes. When DRES i has the p-th highest sensitivity on a regulated node j, the delay time is calculated by $d_{j,i}^{down} = (p-1)\Delta^{delay}$ and $d_{j,i}^{up} = (n-p)\Delta^{delay}$, where Δ^{delay} is the time between two consecutive actions. For voltage reduction, the waiting time of the DRES with highest sensitivity on the regulated node is the shortest.

Max-consensus protocol

The voltage measurement nodes $i \in \{1, \ldots, n\}$ are represented by agents that iteratively share their local information state with their neighbors in order to reach a consensus on the maximum voltage value and the corresponding regulated node. The distributed agents are assumed to measure their local voltage U_i^{loc} in synchronized intervals of Δ^{volt}, e.g., ensured by GPS time or synchronized over the power grid frequency. Each agent i stores its selected maximum voltage value U_i located at a regulated node r_i and a sequence number t_{r_i} in its information state $m_i = (U_i, r_i, t_{r_i})$. Whenever the local voltage updates every Δ^{volt}, the information state is reset to $m_i = (U_i^{loc}, i, t_i + 1)$. Furthermore, due to variable communication delays between agents, asynchronous updates can be triggered by received messages.

Whenever agent i receives a message from agent j, Algorithm 1 is executed. Messages with outdated sequence numbers are ignored; likewise if the regulated node r_j points to agent i. The local information state is updated if voltage U_j is greater than the known one or, in case of equality, only if agent i is a DRES node with higher sensitivity on the regulated node r_j. This ensures nearly optimal overvoltage regulation. Finally, agent i communicates all maximum voltage information states to its neighbors. Thus, every agent can decide individually according to its sensitivity.

Algorithm 1: Process at agent i for received messages form agent j. $communicate(x)$ shares x with its neighbors.

Input: $m_j = \left(U_j, r_j, t_{r_j}\right)$
Data: $m_i = (U_i, r_i, t_{r_i})$
Output: m_i
if $t_{r_j} \geq t_{r_i} \vee r_j \neq i$ **then**
  if $U_j > U_i$ **then**
    $m_i \leftarrow \left(U_j, r_j, t_{r_j}\right)$;
    $communicate(m_i)$; `// only new information state`
  else if $(U_j = U_i)$ **then**
    $communicate(\{m_i, m_j\})$; `// all information states with equal voltage`
    if $(i \leq d) \wedge \left(S_{r_j,i} > S_{r_i,i}\right)$ **then**
      $m_i \leftarrow \left(U_j, r_j, t_{r_j}\right)$;
    end
  end
end

An agent shares its information state with its neighbors whenever (i) the local voltage measurement U^{loc} updates after Δ^{volt}, (ii) a received message updates the local information state m_i, or (iii) a predefined interval $\Delta^{com} < \Delta^{volt}$ has passed. As long as the local voltage values are constant (within Δ^{volt}), eventually all connected agents converge to $U_i = \max_{k\in\{1,\dots,n\}}(U_k^{loc})$. However, agents may point to different regulated nodes, forming consensus clusters depending on their sensitivity.

Communication and overlay network

The communication network is modeled by a static graph $\mathcal{G} = (\mathcal{V}, \mathcal{E})$ consisting of a vertex set $\mathcal{V} = \{1, \dots, m\}$ and a set of edges $\mathcal{E} \subseteq \mathcal{V} \times \mathcal{V}$, including self-loops ($\forall i \in \mathcal{V} : (i,i) \in \mathcal{E}$). Note that at least every agent needs to communicate ($m \geq n$), but additional vertices may exist, such as wireless network base stations. If vertex $i \in \mathcal{V}$ can directly receive information from vertex $j \in \mathcal{V}$, we call i and j neighbors and $(i,j) \in \mathcal{E}$. We assume that bidirectional communication is possible, hence $\mathcal{G}$ is undirected and $\forall (i,j) \in \mathcal{E} : (j,i) \in \mathcal{E}$. The communication delay of messages from i to j can be specified by $d(i,j)$, where $d(i,i) = 0$. Note that communication delay is not necessarily symmetric, hence $d(i,j) = x \not\Rightarrow d(j,i) = x$. We further assume that $\mathcal{G}$ is connected, such that there exist a multi-hop path $(a, \dots, b)$ that connects any two vertices $a, b \in \mathcal{G}$. The communication delay along the path is the sum of the individual communication delays of the neighboring vertices. Finally, we assume that there are no communication failures, as we only investigate the message delay.

An overlay network $\mathcal{G}' = (\mathcal{V}', \mathcal{E}')$ implements logical connections among agents that are placed at a subset of the vertices $\mathcal{V}' = \{1, \dots, n\} \subseteq \mathcal{V}$. Every edge in $\mathcal{E}'$ can be mapped to a path in $\mathcal{G}$, where the one with the smallest expected delay time is chosen in case of ambiguity. The following overlay networks implement different connections $\mathcal{E}'$, where the diameter is given by $D(\mathcal{G}')$.

Local broadcast

A commonly used communication schema for max-consensus algorithms is broadcasting the information state to all direct neighbors (Giannini et al. 2013a, b, 2016; Bertsekas and Tsitsiklis 1989). This overlay network contains all direct edges between agent vertices ($\mathcal{E}' = \{(i,j) \in \mathcal{E} : i,j \in \mathcal{V}'\}$) and transitive edges, that connect two agent vertices from $\mathcal{V}'$ via vertices from $\mathcal{V} \setminus \mathcal{V}'$. The neighbors of agent i are denoted by $\mathcal{N}_i = \{j \in \mathcal{V}' : (i,j) \in \mathcal{E}'\}$. Since broadcast messages will flood the communication network, local information updates (either from local measurement or received messages) are not passed on immediately, but at the next broadcast round after Δ^{com}.

Because messages are only exchanged in synchronized communication intervals Δ^{com}, the system can be seen as synchronous, as long as $\max_{i\in\mathcal{V}', j\in\mathcal{N}_i} d(i,j) < \Delta^{com}$. Asynchronously received messages do not cause any update until the next communication interval, hence can be considered to be synchronously right before the next communication. It is well known, that such a synchronized system converges within $D(\mathcal{G}') \cdot \Delta^{com} < \Delta^{volt}$ (Bertsekas and Tsitsiklis 1989). Some communication technologies support multicast or broadcast messages that address a group or all devices at once. Otherwise, the agents need to send unicast messages to each neighbor individually, which increases the total traffic and overall communication delay.

Static ring

Another simple overlay network is a ring, which connects each agent to exactly two neighbors to form a cyclic path in $\mathcal{V}'$. Because the underlying communication network can have arbitrary topology, neighbors in this path potentially need to communicate via multiple hops in $\mathcal{G}$. However, there exist network embedding algorithms that optimize for minimum communication delay (Wu et al. 2020). In its simplest form, the ring is operated as directed graph, where each agent has only one successor.

Because the global maximum always updates the local information state, the message is immediately re-transmitted to the next agent. Consensus is finally reached when the message fully circled the ring, hence, convergence time scales linearly with the number of agents n. Failing agents cause convergence to fail, however can be detected when no message is received from the predecessor after Δ^{volt} and resolved by skipping the failed agent. Convergence time and failure resilience improve when the ring is operated bidirectionally, which in turn doubles the number of messages.

Sensitivity ring

Instead of embedding the ring with minimum communication cost, the ring can be constructed using the sensitivity matrix of the voltage regulation algorithm. Thereby, the neighbor is selected according to its influence on the locally known regulated node. A non-DRES agent j simply sends its local information state to the DRES agent i with the highest sensitivity on node j, acting as remote measurement devices. If a DRES agent i measures the globally maximum voltage value, it always has the highest sensitivity to its own node i and the next neighbor is the DRES agent with second highest sensitivity. Because the sensitivity matrix is shared among all agents, every DRES agent k that receives (U_i, r_i, t_{r_i}) can assume that agents with higher sensitivity on r_i are already informed and, therefore, communicates to the agent with next lower sensitivity. The ring is closed when agent i receives a message from the lowest sensitive agent on r_i. Because the regulated node changes over time, there exist d different rings (row entries of the sensitivity matrix) that are dynamically chosen depending on the local information state at the sending agent. An exemplary sensitivity ring is depicted in Fig. 2, where the marked row vector of the sensitivity matrix is valid for regulated node 2. The non-DRES agent 5 selects agent 1 from the sensitivity matrix.

Because the overlay sensitivity ring is dynamically chosen, the convergence time is upper limited by the maximum communication delay of the different ring paths plus the maximum delay of the remote measurement devices. The sensitivity ring contains only d DRES agents, which reduces the communication steps required. On the other hand,

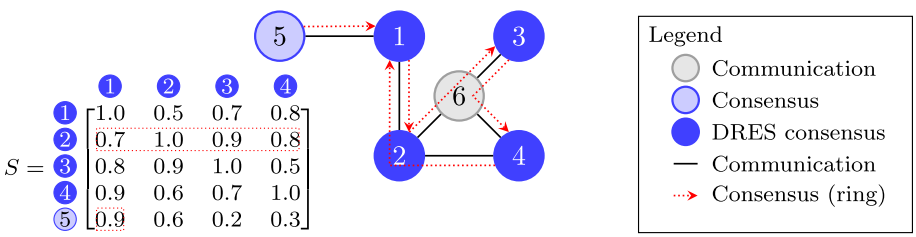

Fig. 2 Example with $m = 6$ communication nodes, $n = 5$ consensus nodes, $d = 4$ DRES nodes depicting the sensitivity ring for regulated node 2

sensitivity rings may have more multi-hop edges, hence, convergence time depends on the underlying communication topology. As one significant advantage, the sensitivity ring guarantees that agents with high sensitivity will obtain updated voltage values much faster, which can speed up the PI controller.

Case study

The proposed max-consensus protocol is applied to a co-simulation scenario with the framework *mosaik* (version 2.5.2) in time resolution of 1 ms. The IEEE 906 low voltage test feeder in Fig. 3 is simplified to a balanced single-phase system simulated by *pypower*.

Consensus agents are located at all 55 household nodes and ideal PV generation profiles are attached at the DRES nodes. The case study demonstrates the impact of communication delay and selection of overlay network on two different communication networks, shown in Fig. 4: (i) A central network $\mathcal{G}_1$ with a wireless base station at the transformer that connects to all agents with bandwidth of 1000 kbit/s ($D(\mathcal{G}_1) = 2$). (ii) A meshed network $\mathcal{G}_2$ that connects any two agents within 40 m with bandwidth of 100 kbit/s ($D(\mathcal{G}_2) = 5$). The message delay along an edge of the communication network consists of four delay parts for *processing*, *queuing*, *propagation*, and *transmission*. Since processing and propagation delays are an order of magnitude smaller than the transmission and queuing delays, we focus on the later two.

Simulation setup

A simple queuing network simulator models the communication network with queues of unlimited size and first-in-first-out logic at every edge. Note that the communication network only depicts logic links between nodes and does not capture additional delays that occur due to packet collisions in the shared medium. A message contains the compressed Internet protocol header (20 Byte), the voltage value as single precision float (4 Byte), the regulated node UUID (16 Byte) and the sequence number as Unix timestamp (4 Byte). In the co-simulation, message delivery is delayed by the calculated

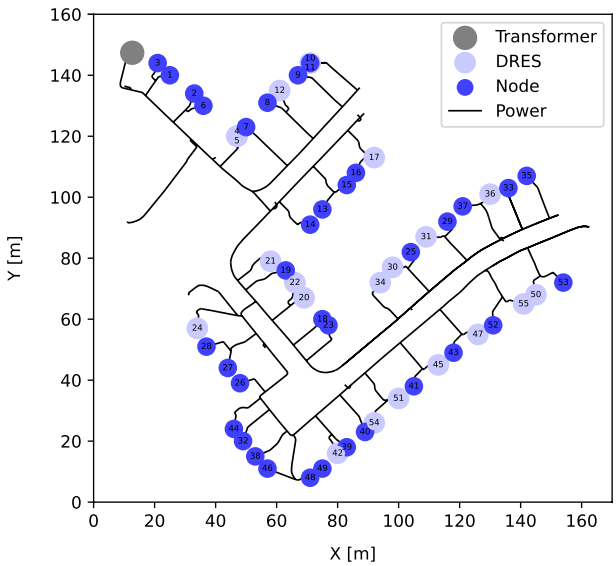

Fig. 3 IEEE 906 low voltage test feeder with 20 DRESs

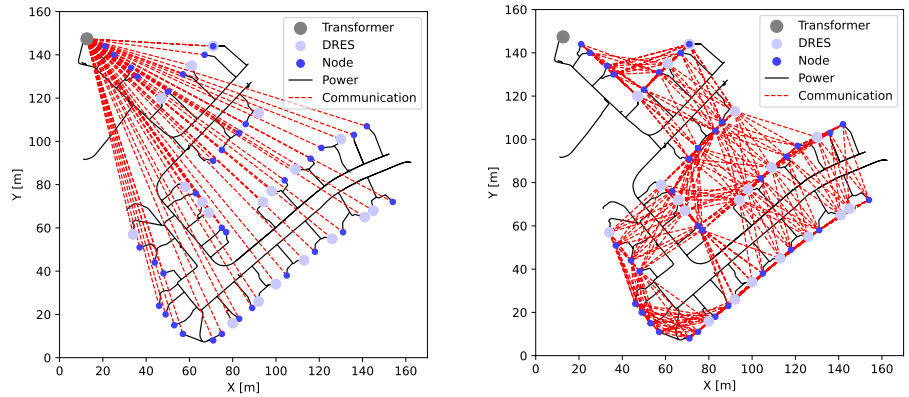

(a) Central communication with a wireless base station at the transformer node, $D(\mathcal{G}_1) = 2$ and bandwidth of 1000 kbit/s, similar to a dedicated 450 MHz LTE network.

(b) Meshed communication with peer-to-peer connections within the range of 40 m, $D(\mathcal{G}_2) = 5$ and bandwidth of 100 kbit/s, similar to a Zigbee network at 868 MHz.

Fig. 4 Communication networks mapped on the IEEE 906 low voltage test feeder

transmission and simulated queuing delay $d(i,j)$ of the path between source i and destination j.

The max-consensus algorithm is compared to a central baseline communication mechanism with a central controller at node 34 that receives all voltage measurements U_i^{loc}, determines the maximum information state every Δ^{com}, and transmits the result to all DRES agents. Note that node 34 is centered in $\mathcal{G}_2$ with minimal total communication hops to all other nodes.

Analysis

The following experiments are executed at 12:00 during the highest PV generation, where household 53 has the unique maximum voltage value and therefore is the regulated node. $\Delta^{volt} = 1$ s is fixed to be greater than the convergence time to avoid voltage changes before a common regulated node is determined.

Using the local broadcast strategy, every agent is reachable via the base station in the central network $\mathcal{G}_1$ ($D(\mathcal{G}_1') = 1$). In the single broadcast round, each agent transmits $54 \cdot 44$ Byte $= 2.376$ kByte and the traffic that passes the base station equals 130.68 kByte. Because all agents communicate at once, Δ^{com} is set to 150 ms, below which $\mathcal{G}_1$ cannot handle the amount of messages. With $D(\mathcal{G}_2) = 5$ and maximum 21 neighbors (mean 13.1) per node, the meshed network $\mathcal{G}_2$ requires 5 broadcast rounds. Despite a 21 % increase of the total traffic ($55 \cdot 5 \cdot 13.1 \cdot 44$ Byte $= 158,51$ kByte), the upper limit passing any vertex is limited by 9.24 kByte. Note that with communication protocols supporting broadcast messages, the required traffic can be reduced. Experimental convergence is shown in Fig. 5.

Ring network embedding on the central communication network $\mathcal{G}_1$ results in two hop communication between any two successive agents, in total 110 hops. However, an optimal ring overlay on the meshed network $\mathcal{G}_2$ has only one hop between any two agents, in total 55 hops. Because a message is transmitted to only one single neighbor at once, the total traffic is rather small. Bidirectional communication in the static ring nearly halves convergence time, as shown in Fig. 6.

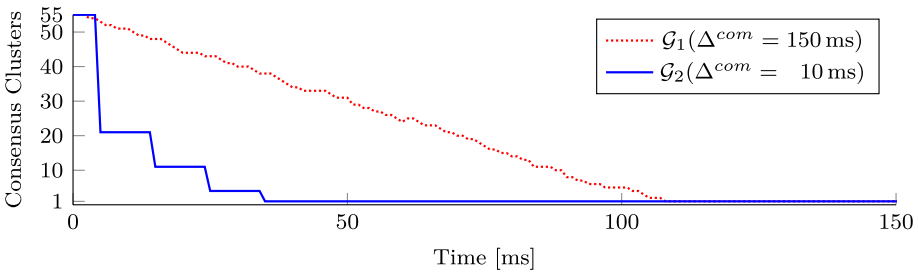

Fig. 5 Convergence time of local broadcast comparing centralized and meshed network

Any sensitivity ring (consisting of the 20 DRES agents) requires 2 hops per agent in $\mathcal{G}_1$ plus 2 hops for each non-DRES agent to reach the most influential DRES agent. Given the sensitivity matrix of the IEEE 906 low voltage test feeder, the sensitivity rings are embedded in $\mathcal{G}_2$ with maximum 40 hops (mean 32.9) and maximum distance of non-DRES agents of 3 (mean 1.2). The sensitivity ring of the regulated node 53 requires only 28 hops in $\mathcal{G}_2$. As can be seen in Fig. 7, the convergence time of the sensitivity ring is reasonable fast, especially on the central network. The total traffic is reduced to 4.88 kByte for $\mathcal{G}_1$ and 7.13 kByte for $\mathcal{G}_2$ due to hierarchical order of remote measurement devices and smaller ring size.

The experiment results are summarized in Table 2, which additionally compares convergence time and traffic requirements with the central baseline algorithm. Similar to local broadcast, the baseline algorithm benefits from meshed networks with no bottleneck at the base station, but represents a single point of failure at the central controller. The sensitivity ring stands out with both, low convergence time and low traffic (total and maximum traffic at a single edge of the communication network). We want to note that with a more realistic network simulator that also covers interference of message delivery

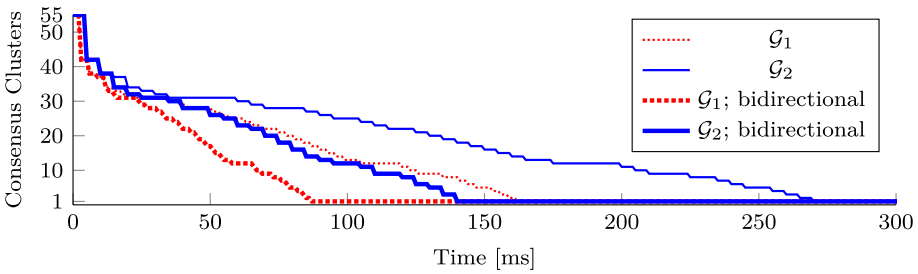

Fig. 6 Convergence time of (bidirectional) ring comparing centralized and meshed network

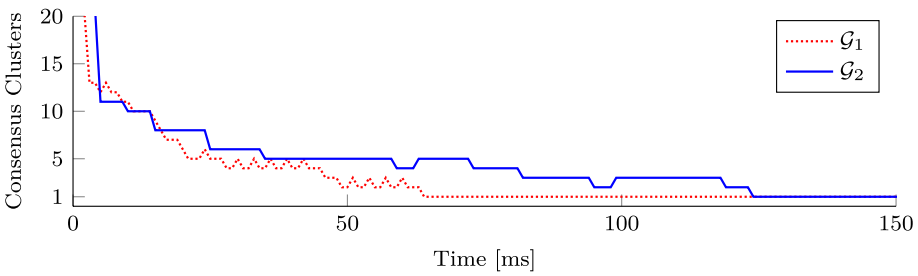

Fig. 7 Convergence time of sensitivity ring for regulated node 53. Note that only the 20 DRES agents need to agree on a consensus

Table 2 Comparison of the different neighbor selection strategies with the central baseline algorithm

	Convergence time (ms)		Total traffic (kByte)		Max edge traffic (kByte)	
	$\mathcal{G}_1$	$\mathcal{G}_2$	$\mathcal{G}_1$	$\mathcal{G}_2$	$\mathcal{G}_1$	$\mathcal{G}_2$
Central baseline	245	97	35.51	12.54	17.56	1.32
Local broadcast	108	50	130.68	158.51	23.76	8.80
Static ring	162	270	20.28	20.28	1.63	0.84
Static ring (bidirectional)	87	140	27.02	26.75	1.63	0.84
Sensitivity ring	64	124	4.88	7.13	1.23	0.62

in the shared medium air, lower traffic is preferred to avoid packet losses and re-transmission, which impacts the message delay and therefore convergence time. However, this also depends on the actual communication technology chosen. The selection of the overlay network is a trade off between convergence time and total traffic, and the optimal decision also depends on the underlying communication network infrastructure.

Conclusion and future work

This paper discussed the problem of determining the maximum voltage value and the corresponding node in the power system using a modified maximum consensus algorithm. Three communication overlay networks are discussed for neighbor selection of each DRES agent. In a case study, the IEEE 906 low voltage test feeder is extended with two communication networks: one with a central base station at the transformer and a meshed network. The simulations show that the optimal overlay network and communication strategy depends on the underlying communication infrastructure and is trade off between convergence time and total required traffic. Local broadcasting works fast in meshed communication networks with reasonable low amount of required traffic per edge. However, central communication networks work best with ring overlay network, where especially the sensitivity ring can drastically reduce the required traffic.

In the future, this work will be extended with an exact communication simulation that considers packet interference in shared media. Furthermore, it is planned to investigate the impact of failures and to perform a closed loop evaluation to identify the impact of the consensus mechanism on the voltage regulation algorithm.

About this supplement
This article has been published as part of Energy Informatics Volume 5 Supplement 1, 2022: Proceedings of the 11th DACH+ Conference on Energy Informatics. The full contents of the supplement are available online at https://energyinformatics.springeropen.com/articles/supplements/volume-5-supplement-1.

Author contributions
DD contributed the idea, max-consensus algorithm as well as the evaluation setup and analysis. He also wrote the first draft of the paper. HdM provided research direction, supervision, and helped to write the final version of the paper. Both authors read and approved the final manuscript.

Funding
This project has received funding from the European Union's Horizon 2020 research and innovation programme under grant agreement No. 957845: "Community-empowered Sustainable Multi-Vector Energy Islands - RENergetic".

Availability of data and materials
The co-simulation environment with all connected simulators and results are available from the corresponding author on reasonable request.

Declarations

Competing interests
The authors declare that they have no competing interests.

Published: 7 September 2022

References

Bertsekas DP, Tsitsiklis JN (1989) Parallel and distributed computation: numerical methods. Prentice-Hall Inc, Hoboken. https://dl.acm.org/doi/abs/10.5555/59912

Brenna M, De Berardinis E, Delli Carpini L, Foiadelli F, Paulon P, Petroni P, Sapienza G, Scrosati G, Zaninelli D (2013) Automatic distributed voltage control algorithm in smart grids applications. IEEE Trans Smart Grid 4(2):877–885. https://doi.org/10.1109/TSG.2012.2206412

Deplano D, Franceschelli M, Giua A (2020) Dynamic max-consensus and size estimation of anonymous multi-agent networks

Faiya BA, Athanasiadis D, Chen M, McArthur S, Kockar I, Lu H, de León F (2021) A self-organizing multi-agent system for distributed voltage regulation. IEEE Trans Smart Grid 12(5):4102–4112. https://doi.org/10.1109/TSG.2021.3070783

Giannini S, Di Paola D, Petitti A, Rizzo A (2013) On the convergence of the max-consensus protocol with asynchronous updates. In: 52nd IEEE conference on decision and control, pp 2605–2610

Giannini S, Petitti A, Di Paola D, Rizzo A (2013) Asynchronous consensus-based distributed target tracking. In: 52nd IEEE conference on decision and control, pp 2006–2011

Giannini S, Petitti A, Di Paola D, Rizzo A (2016) Asynchronous max-consensus protocol with time delays: convergence results and applications. IEEE Trans Circuits Syst I: Regul Pap 63(2):256–264. https://doi.org/10.1109/TCSI.2015.2512721

Hu Q, Bu S (2021) A distributed p and q provision based voltage regulation scheme by incentivized ev fleet charging for resistive distribution networks. IEEE Trans Transp Electrif 7(4):2376–2389. https://doi.org/10.1109/TTE.2021.3068270

Iutzeler F, Ciblat P, Jakubowicz J (2012) Analysis of max-consensus algorithms in wireless channels. IEEE Trans Signal Process 60(11):6103–6107. https://doi.org/10.1109/TSP.2012.2211593

Kontis EO, Kryonidis GC, Nousdilis AI, Malamaki K-ND, Papagiannis GK (2019) A two-layer control strategy for voltage regulation of active unbalanced lv distribution networks. Int J Electr Power Energy Syst 111:216–230. https://doi.org/10.1016/j.ijepes.2019.04.020

Kryonidis GC, Demoulias CS, Papagiannis GK (2016) A nearly decentralized voltage regulation algorithm for loss minimization in radial mv networks with high dg penetration. IEEE Trans Sustain Energy 7(4):1430–1439. https://doi.org/10.1109/TSTE.2016.2556009

Kryonidis GC, Kontis EO, Chrysochos AI, Demoulias CS, Papagiannis GK (2018) A coordinated droop control strategy for overvoltage mitigation in active distribution networks. IEEE Trans Smart Grid 9(5):5260–5270. https://doi.org/10.1109/TSG.2017.2685686

Kryonidis GC, Demoulias CS, Papagiannis GK (2019) A new voltage control scheme for active medium-voltage (mv) networks. Electr Power Syst Res 169:53–64. https://doi.org/10.1109/TSG.2017.2685686

Kryonidis GC, Demoulias CS, Papagiannis GK (2020) A two-stage solution to the bi-objective optimal voltage regulation problem. IEEE Trans Sustain Energy 11(2):928–937. https://doi.org/10.1109/TSTE.2019.2914063

Kryonidis GC, Malamaki K-ND, Gkavanoudis SI, Oureilidis KO, Kontis EO, Mauricio JM, Maza-Ortega JM, Demoulias CS (2021) Distributed reactive power control scheme for the voltage regulation of unbalanced lv grids. IEEE Trans Sustain Energy 12(2):1301–1310. https://doi.org/10.1109/TSTE.2020.3042855

Lin J, Morse AS, Anderson BD (2007) The multi-agent rendezvous problem. Part 2: The asynchronous case. SIAM J Control Optim 46(6):2120–2147. https://doi.org/10.1137/040620564

Millar BS, Jiang D (2018) Asynchronous consensus for optimal power flow control in smart grid with zero power mismatch. J Mod Power Syst Clean Energy 6(3):412–422. https://doi.org/10.1007/s40565-018-0378-4

Monteiro JC, Peixoto AJ (2020) Convergence and stability properties of a dynamic maximum consensus estimator. IFAC-PapersOnLine, 21st IFAC World Congress 53(2):2885–2890

Nejad BM, Attia SA, Raisch J (2009) Max-consensus in a max-plus algebraic setting: the case of fixed communication topologies. In: 2009 XXII international symposium on information, communication and automation technologies, pp 1–7

Rousis AO, Tzelepis D, Pipelzadeh Y, Strbac G, Booth CD, Green TC (2021) Provision of voltage ancillary services through enhanced tso-dso interaction and aggregated distributed energy resources. IEEE Trans Sustain Energy 12(2):897–908. https://doi.org/10.1109/TSTE.2020.3024278

Shi G, Xia W, Johansson KH (2015) Convergence of max-min consensus algorithms. Automatica 62:11–17. https://doi.org/10.1016/j.automatica.2015.09.012

Wang D, Meng K, Gao X, Qiu J, Lai LL, Dong ZY (2018) Coordinated dispatch of virtual energy storage systems in lv grids for voltage regulation. IEEE Trans Ind Inform 14(6):2452–2462. https://doi.org/10.1109/TII.2017.2769452

Wu H, Zhou F, Chen Y, Zhang R (2020) On virtual network embedding: Paths and cycles. IEEE Trans Netw Serv Manag 17(3):1487–1500. https://doi.org/10.1109/MASCOTS.2019.00027

Zhang S, Tepedelenlioğlu C, Banavar MK, Spanias A (2016) Max consensus in sensor networks: non-linear bounded transmission and additive noise. IEEE Sens J 16(24):9089–9098. https://doi.org/10.1109/JSEN.2016.2612642

Publisher's Note